Virtual Instrumentation for Time-Domain Active and Reactive Power Measurement and Compensation in Industrial Networks

Florin Sandu, Iuliu Szekely, Wilibald Szabo, Gheorghe Scutaru

"Transilvania" University, Bulevardul Eroilor 29A, Brasov, 500036, Romania, tel&fax +40268478705
e-mail: sandu@unitbv.ro , szekelyi@vega.unitbv.ro , szabo@unitbv.ro , scutaru@unitbv.ro

Abstract- The authors implemented power measurement methods in non-sinusoidal regime using an original in-time signal processing: the temporal active power formula, applied to a pair of periodic signals representing voltage and current can be applied also to current (as it is) and Hilbert transform of voltage (kept in time domain) to compute the reactive power. The suggested algorithms were oriented towards digital signal acquisition and processing; their efficiency was compared with traditional methods and also with the implementation alternatives. Sampling rate was synchronized with the signal, as most industrial power meters don't require a time reference (the power values are normalized to the period of the signal). The virtual instruments accomplished are directly applicable in real time monitoring and reactive power compensation for non-sinusoidal regime using recent developments in the technology of capacitors.

I. Introduction

Last years' progress in power electronics is accompanied by a world-wide spread of deforming receivers that are responsible of voltage and current harmonics appearing in electrical energy distribution networks. Deforming regime in an electro-energetic system has a negative impact on efficiency and cost of electrical energy transportation, over a range of equipment that is sensitive to deformation of voltage and current.
Based on the classic definitions of C. Budeanu [1], we implemented some power measurement methods in non-sinusoidal regime using an original in time signal processing. New formulas recommended by other authors can be easily implemented as well.
The suggested algorithms are oriented towards digital signal acquisition and processing; their efficiency is compared with traditional methods and also with the implementation choices. The temporal active power formula, applied to a pair of periodic signals representing voltage and current can be applied also to current (as it is) and Hilbert transform of voltage (kept in time domain) to compute the reactive power. Specific computational aspects are compared with traditional methods. There are described hardware and software implementations of the suggested method, by digital signal processors, field programmable gate arrays and data acquisition-based virtual instrumentation. The control clock is PLL synchronized with the acquired signal, to obtain a maximum of accuracy with economic implementations. In the second part of the paper, the specific algorithms are extended towards the compensation of inductive-generated reactive power by adaptive adjustment of capacitor (binary-weighted) banks.

2. Overview of Standard Formulas for Power Computation

The well-known formulas of non-sinusoidal periodical regime specific active (P) and reactive (Q) powers are [1]:

$$P = \frac{1}{T} \cdot \int_0^T u(t) \cdot i(t) \cdot \mathrm{d}t = \sum_{k=0}^{\infty} U_k \cdot I_k \cdot \cos \varphi_k \qquad (1),$$

where T is the period, u , i and U_k , I_k are the voltage and current, in temporal and, respectively, in spectral (Fourier series harmonics of index k) representations (φ_k is the phase difference between the k^{th} harmonics of voltage and of current).

$$Q = \sum_{k=0}^{\infty} U_k \cdot I_k \cdot \sin \varphi_k \qquad (2);$$

To complete these calculations, it is obviously needed to compute the spectral components, both for the current and voltage, amplitudes and phases - at least φ_k – or real and imaginary parts of the harmonics (spectral decomposition, in "waves", is relevant more or less for such signals only). These complex numbers calculations, needed for both voltage and current, recommend an alternative set of exclusively temporal formulas to be more computationally efficient (considering that *u* and *i* have real values).
As described in their papers [4] and [5], the authors implemented the following formula of the reactive power:

$$Q = \frac{1}{T} \cdot \int_0^T u(t) \cdot \mathrm{H}\{i\}(t) \cdot \mathrm{d}t = -\frac{1}{T} \cdot \int_0^T \mathrm{H}\{u\}(t) \cdot i(t) \cdot \mathrm{d}t \quad (3),$$

where $\mathrm{H}\{u\}(t)$ is the Hilbert transform of the voltage *u(t)* etc. Since the Hilbert transformer is a broad-band phase shifter with $\pi/2$ (for each pulsation ω, the spectral line of the Hilbert transform keeps the module but is phase shifted by $-\pi/2$), then $Q(u,i) = P(u,\mathrm{H}\{i\}) = -P(\mathrm{H}\{u\},i)$, because $\sin\varphi_k$ for $(u,\mathrm{H}\{i\})$ equals $\cos\varphi_k$ for *(u, i)* etc.

Compared to the Fourier transform of a signal $x(t)$, $\mathrm{F}\{x\}(\omega) = \int_{-\infty}^{+\infty} x(t) \cdot \mathrm{e}^{-\mathrm{j}\omega t} \cdot \mathrm{d}t$ the Hilbert transform $\mathrm{H}\{x\}(t) = \frac{1}{\pi} \cdot \left(\begin{matrix} \text{principal} \\ \text{value} \end{matrix} \right) \int_{-\infty}^{+\infty} \frac{x(t)}{t - \tau} \cdot \mathrm{d}\tau$ that is the convolution with the weighting function of the Hilbert transform (that represents IFT, the inverse Fourier transform, of signum (ω)):

- doesn't need calculation with complex numbers and
- keeps the signal in the time domain - then, (to be combined with this transform, being in the same domain) the other signal can remain in time domain as it is:
- the transform is applied only to one signal (current or, more often, voltage – since it is less deformed).

3. Discrete Time Computations

The spread of data acquisition (DAQ) systems in modern measurement puts the emphasize on discrete time computations.
The discrete time formulas corresponding to (1) and (3) are, with N being the period of acquired sequences $\{i_n\}$ and $\{u_n\}$,

$$P = \frac{1}{N} \cdot \sum_{n=0}^{N-1} u_n \cdot i_n \quad (4);$$

$$Q = -\frac{1}{N} \cdot \sum_{n=0}^{N-1} i_n \cdot \mathrm{H}\{u\}_n \quad (5).$$

Since the signals are periodic the Hilbert transform is done by cyclic convolution with the weighting sequence $\mathrm{h}_n = \text{Discrete IFT}\{ \overbrace{\mathrm{S}_k}^{-\operatorname{signum}(k - \frac{N}{2})} \} = \begin{cases} 0 & \text{for even } n \\ \frac{2}{N} \cdot \operatorname{cotan} \frac{n \cdot \pi}{N} & \text{for odd } n \end{cases}$. It results:

$$\mathrm{H}\{u\}_n = \sum_{m=0}^{N-1} \mathrm{h}_m \cdot u_{n-m} \quad (6).$$

There are some disadvantages specific to simple convolution of periodic signals. To reduce the edge errors, there are needed long acquisition times, lasting more times than only *T,* the period of the continuos signal to be sampled and acquired. Windowing is also required, with complicate temporal weighting, more or less adapted to the signal. To compute the "periodograms", for instance, there are usually hundreds or thousands of samples needed, divided in sub-sequences, with or without averaging or overlapping etc. [4].
A problem to be solved, both for the precision of Fourier and Hilbert transforms of periodic sequences by cyclic convolution, is the need for a perfect match between the period of the signal and the length of the considered convolution cycle.

This is usually the finite length of the acquisition window that represents exactly one signal's period (or, sometimes, a multiple of it).
As regarding N , there is no need of a too great temporal resolution - according to Nyquist theorem, N doesn't need to be much greater than double the (expected) index of the highest signal's harmonic. For efficient algorithms of discrete Fourier (Cooley-Tuckey) transforms, N is often a power of 2. There are also efficient algorithms for the fast Hilbert transform that exploit specific properties beginning with the symmetry of Hilbert weighting sequence and with the fact that half of weighting coefficients are 0.
Concluding, the advantages of cyclic convolution are:
- short acquisitions, that could last only one period;
- no need of windowing.

4. Synchronisation of the Sampling Rate

As presented above, adapting of the sampling period T_{CLK} to the signal's period T , providing $T=N \cdot T_{CLK}$ has the advantage of a reduced sampling frequency and, mainly, of increased accuracy of cyclic convolution computations.
This synchronisation was implemented by the authors by means of a hardware PLL (phase locked loop) that was configured for frequency multiplication (then with a frequency divider by N in its feed-back), with the signal (e.g. voltage) as input and its sampling clock as output.
The principle of this synchronisation takes advantage of an important property of power formulas (1) and (5): since the result is divided by T, there is no need for a time unit of reference! So, the sampling period can be not fixed but adapted to the signal.

5. Virtual Instrumentation – Implementation of Adaptive Varmeters / Wattmeters for Industrial Frequencies

All the systems presented take benefit of an adaptive clock. The control clock was synchronised by a LM565–PLL with a CA4020 counter in its feed-back. For industrial network signals, it can be admitted by these means a fundamental frequency fluctuation of at least ± 20 % (relative to the standard value of 50 Hz or 60 Hz).

A. Virtual wattmeter/varmeter

The hardware of this National Instruments (NI) implementation (fig.1) was based on AT-MIO-16E-10 data acquisition board, driven by LabView™ software.
The synchronisation auxiliary circuits provide the exterior clock taken to control the sampling.
The panel of this virtual instrument allows the user to choose the input channels, the number of samples to be acquired, the control input (and the control edge of pulses) and displays the waveforms of $\{i\}$, $\{u\}$ and $H\{u\}$, together with the computed values of the active and reactive power. The diagram of the virtual instrument (VI) was designed with the visual programming tools of LabView. Besides the general blocks for any acquisition VI, the particular parts, presented according to signals' fluency through the processing blocks, are doing the reshape (rearranging) of the acquired samples' table and decimation of the obtained line vector, separating as samples with even index 0, 2, 4, ... those of current and as samples with odd index 1, 3, 5, ... those of voltage.
This general purpose DAQ board does sequential (not simultaneous) sampling of the inputs, so there are acquired 64+64 interleaved voltage and current samples per period. A specific feature of this implementation is then the linear interpolation of 1-st order accomplished for each pair of consecutive voltage samples in order to approximately compute the voltage value that was simultaneous to that of the intermediate current sample. This is done by cyclic permutation - rotation to the left with one position (parameter –1) of the voltage sequence (index 1, 3, 5, ... become -1, 1, 3, ... in order that their half-summation with index 1, 3, 5, ... should deliver just the index 0, 2, 4, ... To reduce to a minimum the approximation errors, this interpolation (as well as the Hilbert transform) is applied to the less deformed signal (usually the voltage).
The active and reactive powers are computed through dot (by dot) product of (interpolated) $\{u\}$ and $\{i\}$ sequences, respectively of $\{i\}$ and $H\{u\}$. The present implementation, for active and reactive power measurement, involves a sampling clock synchronization so that $T = N \cdot T_{sampling}$ with $N = 64$. The value chosen for N covers (according to the Nyquist criterion) signals with less than $N / 2 = 32$ important harmonics; similar wattmeters / varmeters implemented for industrial frequencies take into consideration a maximum of 11-13 harmonics.

B. Implementation in a configuration delivered by National Instruments

The system used to implement the previous formulas is presented in fig. 1.

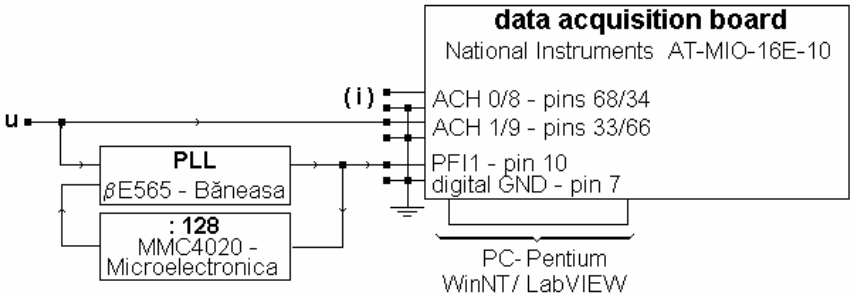

Fig. 1 – Computer controlled DAQ and processing system for the measurement of active and reactive powers – dedicated to industrial frequencies
(PLL is tuned at the free oscillation frequency of 128 x 50 Hz = 6,4 kHz at the output)

Together with the main software component, the LabView package, the specific hardware component is the acquisition board AT-MIO-16E-10 that, among the multiple input / output modes (**M**ultiple **I**nput/**O**utput), allows an exterior sampling clock, offered here by the PLL, so there are acquired exactly 64 samples / period [= 128: (number of channels)]. AT-MIO-16E10 is totally software configurable by the "panel" created in LabView context for displays and user controls (fig. 2).

The board is of "plug-and-play" type (without any on-board switch), so the user must set mainly:
- the number of the board (1) in system controlled by LabView
- the numbers of the channels (0 and 1 in fig.1, 2 and 5 in fig.2 etc.) for the current and voltage [the board has 16 unipolar channels, configurable also as 8 bipolar channels - as in the present case, when the proper voltage *{ u }* and the voltage the current *{ i }* was converted in (the converter may be even a simple shunt, because the board "reads" analog signals as voltages, on very large input resistors) have practically an alternative variation, on both sides of 0] ; unfortunately, the used board doesn't sample simultaneously more channels, but interleaved, with time division (the interleave factor corresponds to the programmed number of channels, being here 2).
- the number of samples sets (a "*n*-uple", where *n* is the number of channels ; in this case there are then 64 pairs)
- the time limit - to wait the so specified number of sampling pulses (sampling could generally be non-uniform) ; here, after the 5 programmed seconds, the "time over" flag turns red.
- the code of the input where the sampling clock is brought (it was used one of the 10 PFI - "Programmable Function Inputs") ; it was chosen PFI1, with the sampling moment on the "low-to-high" front of PLL out pulses.

The display includes:
- graphs to observe the correct operation *[{ u , i }* and *H { u }*
- the numeric value (in V^2) corresponding to the active and reactive power [correctable to the proper values by dividing, as example, to the number (64) of sample pairs *{ u , i }* and at the resistance of the shunt that converts the current also in a voltage.

Visual programming (a strong feature of LabView) of the system was done by the diagram of fig. 3.

The central and inferior part of the diagram in fig.3 is a virtual sub-system "ExtChanClk", available in the set of "Virtual Instruments" (**.**VI) of LabView package, for data acquisition appliances with analog inputs, with an exterior clock taken through a channel of the board ["DAQ (Digital Acquisition) Applications / Analog Input / Exterior-Channel Clock"].
The specific sub-systems of this configuration are positioned in the right-superior part of the diagram. The most important will be described in the order of signals' fluence through the computation blocks:

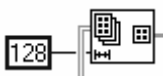

"**Reshape** (rearranging of the) **Array**" with *n* lines (*n* = channels number, here *n*=2) and with a columns number equal with the number of sets [n - ples, here pairs *(u, i)*] measured, that contain the acquired values as a vector line vector with 128 = 2 x 64 interleaved values.


"**Decimate**" of the obtained line vector, separating as samples with even index 0, 2, 4 … those of current and as samples with odd index 1, 3, 5 … those of voltage.

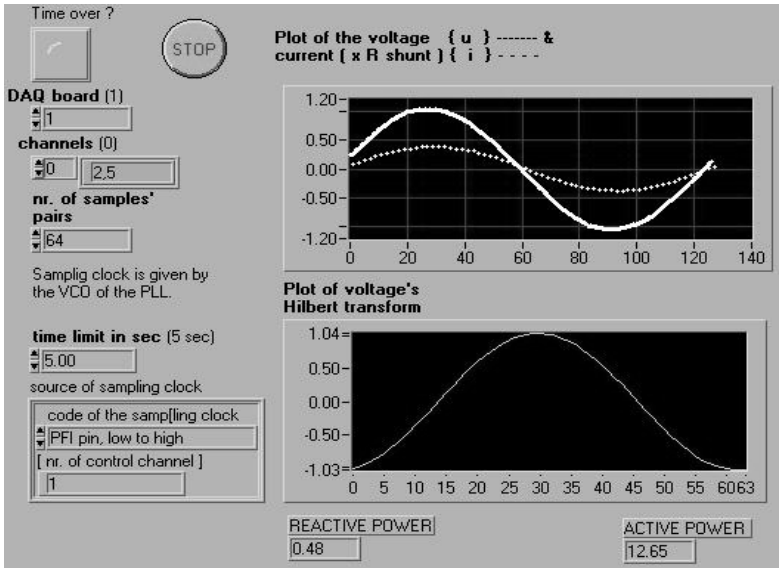

Fig. 2 – LabView panel for displays and user programmed controls

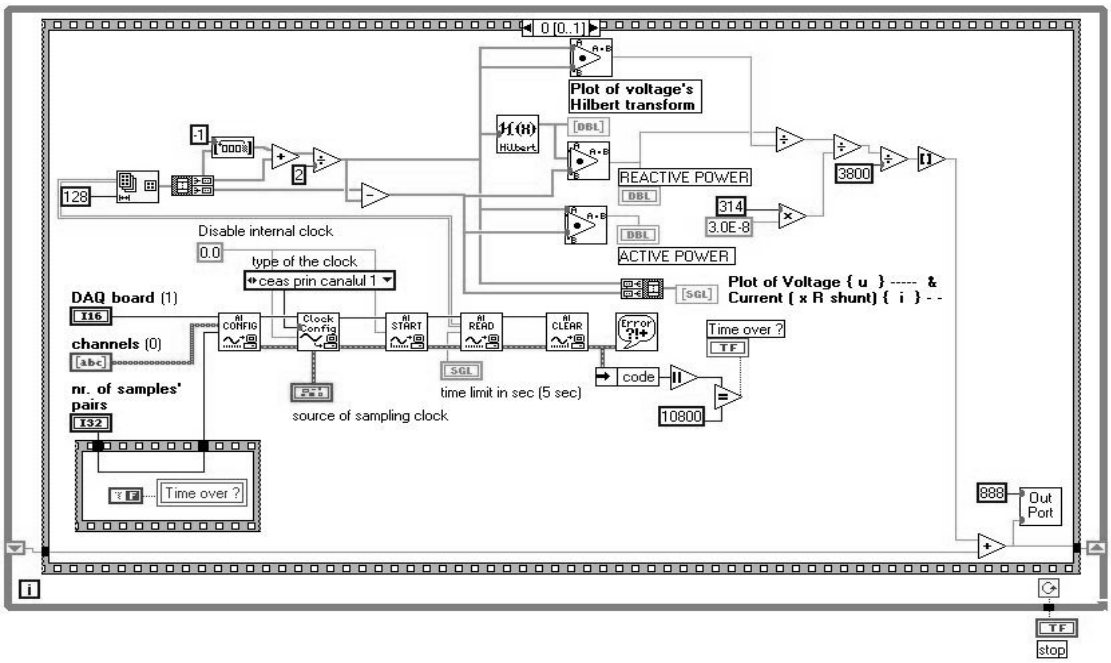

Fig. 3 – The LabView diagram of the system


Cyclic permutation - rotation (**"Rotate"**) to the left with one position (parameter –1) of voltage sequence (index 1, 3, 5, ... become -1, 1, 3, ... in order that their **half-summation** with index 1, 3, 5, ... should deliver just the index 0, 2, 4, ... This allows the approximate computation, by linear interpolation of first order**,** of voltage samples which would correspond exactly to the moment when those of current are acquired. To reduce to a minimum the approximation errors, this interpolation (as well as the Hilbert transform) is applied to the less deformed signal (usually the voltage).

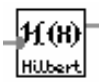
Hilbert transform (of corrected voltage) block


"Dot (by dot) **Product"** of (corrected) *{ u }* and *{ i }* sequences (then $[u]\cdot[i]^T$), respectively of *{ i }* and *H { u }*, to compute the active, respectively reactive power

6. Real-Time Reactive Power Compensation.

The implemented virtual instrument can run in a *loop of repetitive acquisition & processing*, so fast as it is appropriate for operative control and even for real time compensation of any deformant effects and, mainly, of phase shifts - as most legislative systems state the requirement that the industrial enterprise producing any reactive load in the distribution network is responsible of its local compensation. In the 2nd frame of the diagram, a simple 1s delay was introduced. This delay, with an appropriate magnitude order lower than the time-constant of the industrial process compensated (e.g. Siemens-Martin induction metallurgic ovens etc.) can be programmed (being enough for relay-based switching of compensation capacitors' arrays).

The successful experiments with the system described in paragraph 5, encouraged the authors to consider its development for real-time reactive power compensation approach. The simplified compensation probe is given in fig. 4:

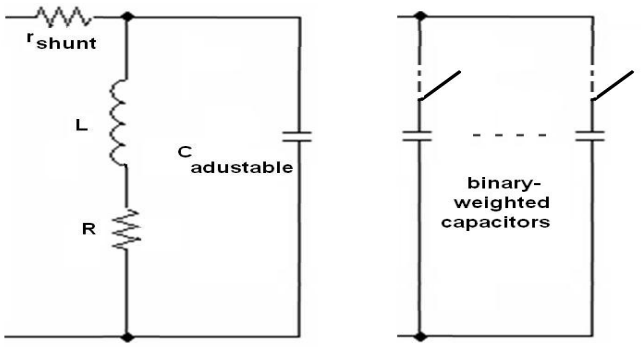

Fig. 4. Compensation probe: the adjustable *C* compensates a main load, *R*, with own inductance, *L*

It was used a *mobile core* inductor (4,1 to 14,6 F) with a resistance *R* of 7,5 kΩ. The "shunt" resistor was chosen with a particular value of 3,8 kΩ (for comparable ranges of acquired voltages) – nevertheless, its value should be adequate smaller in practice but this was considered beyond the simplified requirements of the test-bench (fig.5):

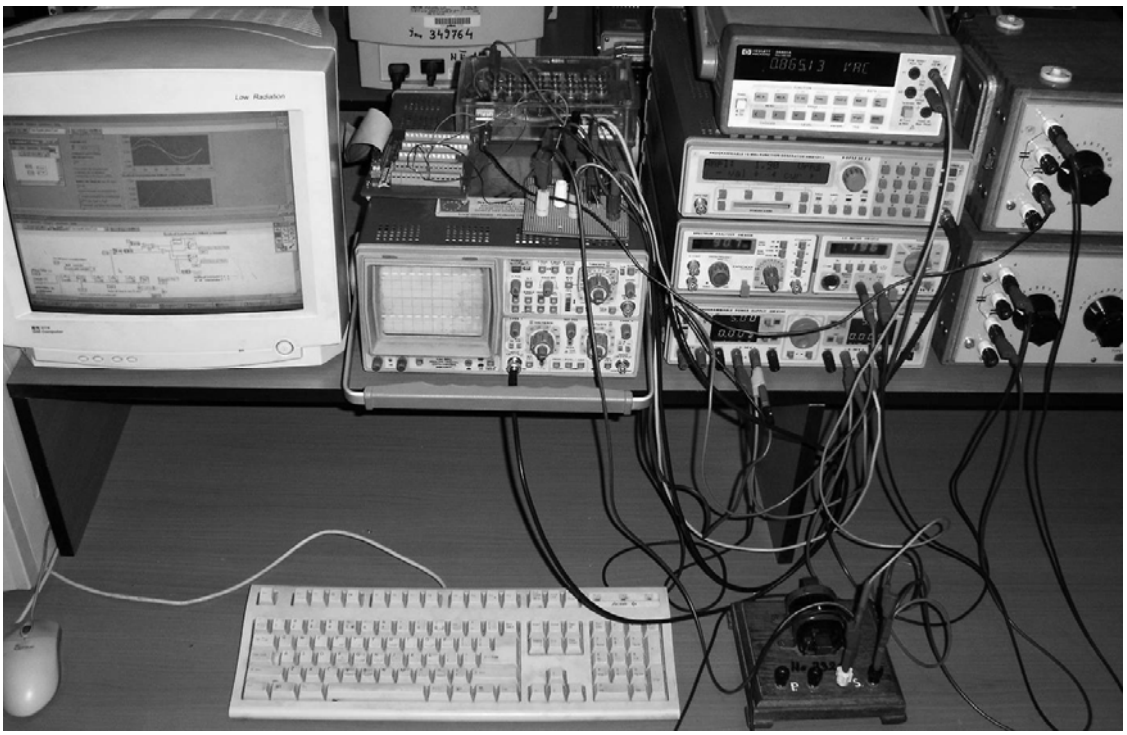

Fig. 5 The work-bench: over the Digital Oscilloscope – HAMEG, HM1007 (in front left), is the junction board of AT-MIO16E10; front-right is the PLL circuit and in the rear the Relay Box (see fig.4 and fig.6). The tower on the right includes (top-down) the Digital Multimeter (DMM) Hewlett Packard, HP34401A, the Function Generator – HAMEG, HM8131, the RLC bridge (and spectral analyzer) (HAMEG HM8028 modular system), the Power Supply HAMEG, HM8442 and the Calibrated Decade Capacitors (binary adjusted to 30nF, 60nF, 120nF).

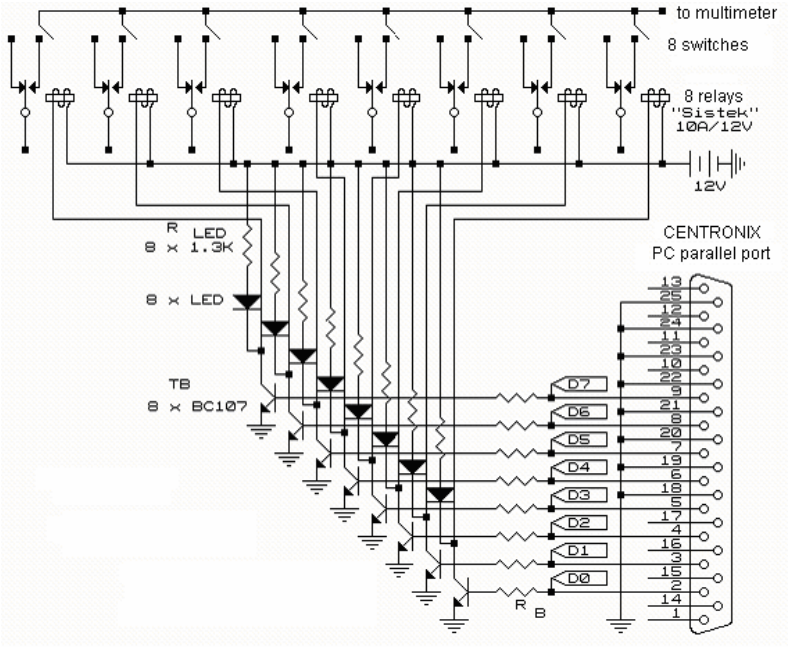

Fig. 6 The relay bench controlled via Centronics (LPT) parallel port

The software control of relays bench is very simple: writing to the Centronics (LPT) parallel port having the address $378_{(16)}$ ($= 888_{(10)}$) of the word $01010111_{(2)} = 57_{(16} = 87_{(10)}$ (for example) is accomplished with LabView control:

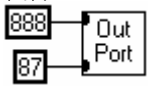

If C is built out of binary-weighted capacitors (best compromise of both resolution and dynamic range) the computed decimal number (e.g. 87) is fed as C adjustable / (last-significant) C.

The compensation capacitor introduced in the circuit is computed according to the following formulas (considered for $f \approx 50\text{Hz}$):

The parallel-grouped conductance $\mathrm{j}\omega C + \dfrac{1}{R + \mathrm{j}\omega L}$ is real for $C = \dfrac{L}{R^2 + \omega^2 \cdot L^2}$.

In this case, the overall impedance has the real value $R + \dfrac{\omega^2 \cdot L^2}{R}$ (= 10.3 kΩ for R = 7.5 kΩ and L = 14.6 H, when the compensation capacitance is C = 189 nF).

The virtual instrument computes, for negative / positive P_r , *decrease / increase* of the compensation capacitor (assuming that fundamental is predominant in comparison with continuous and harmonic components).

$$C = \frac{\sum_{n=0}^{N-1} i_n \cdot \mathrm{H}\{u\}_n}{\sum_{n=0}^{N-1} {u_n}^2} \cdot \frac{1}{2\pi \cdot \underbrace{50\text{Hz}}_{\text{estimated } f}}$$

Indeed, for resistive load (R), with series inductance (L), the compensation capacitance:

$$C = \left(\frac{\omega \cdot L}{R^2 + \omega^2 \cdot L^2} \right) \cdot \frac{1}{\omega_{estimated}} \approx \frac{\sin \varphi_1 \cdot |Z|}{|Z|^2} \cdot \frac{1}{\omega_{estimated}}$$

Instant value of capacitance is cumulated with previous one brought from the beforehand execution instance via *shift-registers* added to sequence frames in the VI *Case* loop.

Case study: for U_{in} = 1 V RMS, the DMM measures U = 733 mV_{RMS} (one can verify it by voltage divider rule: $1000\text{mV} \cdot \frac{10.3\text{k}\Omega}{10.3\text{k}\Omega + 3.8\text{k}\Omega} = 733\text{mV}$); the virtual instrument plots a voltage with 1.04 $V_{amplitude}$ (= 733 mV_{RMS} $\cdot\sqrt{2}$) and a current (x R_{shunt}) = 267 mV_{RMS} = 378 $mV_{amplitude}$ The active power in the compensated group is measured as $12.65V^2$ (that can be verified, considering scaling constants, as $\underbrace{64}_{\substack{\text{samples /}\\ \text{period}}} \cdot \underbrace{3.8\text{k}\Omega}_{R_{shunt}} \cdot (733\text{mV})^2 / \underbrace{10.3\text{k}\Omega}_{Z\,(real)}$).

Without compensation *C*, one can check the reactive power (x 64 x R_{shunt}) = $7.7V^2$ (= $\frac{\omega L}{R} \cdot 12.65V^2$).

Compensation example:

$$Q_c = P_C\left(\text{tg}\,\varphi_1 - \text{tg}\,\varphi_2\right)$$

$\cos\varphi_1$ - natural power factor

$\cos\varphi_2$ - neutral power factor (0.92)

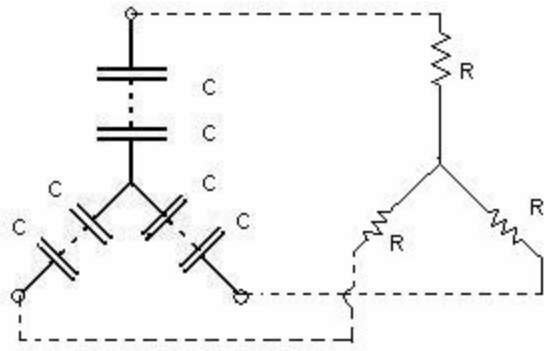

Reactive power of the compensation capacitor (e.g. C=12F , U_n=110V):

$$Q = \frac{U_n^2}{\frac{1}{\omega c}} = \omega c U_n^2 = 314 \cdot 12 \cdot 110^2 = 45.6MVAR$$

Total reactive power of the capacitor banks:

$$Q_t = 6 \cdot Q = 273.6MVAR$$

With these 6 capacitors we can increase the power factor from 0.75 to 0.92 for desired active power.

$$P_c = \frac{Q_t}{T_g\varphi_1 - T_g\varphi_2} = \frac{273.6}{0.456} = 600MW$$

Computing the discharge resistors :

$$R = \frac{t_d}{\frac{C_n}{2}\ln\frac{U_f\sqrt{2}}{U_{adm}}} = \frac{60}{6\ln\frac{220\sqrt{2}}{42}} = 5\Omega$$

7. Conclusions

The application of the Hilbert transform to active and reactive power measurement brought practically all the required digital signal processing in time domain.
Economic implementations took benefit of sampling rate synchronization with the signal.
The presented solutions can be applied in computer controlled, real time monitoring and compensation of non-sinusoidal regime using the recent developments in capacitor technologies.

References

[1] C.I. Budeanu, “Reactive and fictive powers” ("Puissances reactives et fictives"), *Journal of the Romanian institute of energy*, Bucharest, Romania, 1927

[2] Z. Nowomiejski, “Generalized theory of electric power”, *Archiv für Elektrotechnik,* vol.63, 1981

[3] S. Mitra *Digital signal processing,* McGraw Hill, 2001

[4] F. Sandu, W. Szabo, D. Ursuțiu, "Virtual Instrumentation for Power Measurement at Industrial Frequencies, in *"Proceedings of the 6th International Conference on Optimization of Electric and Electronic Equipments - OPTIM'98"*, Braşov, Romania

[5] F. Sandu, W. Szabo, "Time-domain Signal Processing for Power Measurement in Industrial Networks", in *“Proceedings of la X IMEKO TC-4 SYMPOSIUM"*, Naples, Italy, 17–18 sept. 1998.